

PAP-885

TECHNICAL SERVICE CENTER
Denver, Colorado

Technical Memorandum No. Hv-D8560-2001-1

Lower Colorado
Boulder Canyon
Hoover Dam Penstock System
Evaluation of tie rods at the A-1 penstock junction,
Upper Arizona Penstock

Prepared by

K. Warren Frizell
and
Joseph P. Kubitschek

U.S. Department of the Interior
Bureau of Reclamation

Technical Service Center
Denver, Colorado



October 2001

UNITED STATES DEPARTMENT OF THE INTERIOR

The mission of the Department of the Interior
is to protect and provide access to our
Nation's natural and cultural heritage and
honor our trust responsibilities to tribes.

BUREAU OF RECLAMATION

The mission of the Bureau of Reclamation
is to manage, develop, and protect water
and related resources in an environmentally and
economically sound manner in the interest
of the American public.



BUREAU OF RECLAMATION

Technical Service Center, Denver, Colorado

Technical Memorandum No. HV-D-8560-2001-1

Region: Lower Colorado

Project: Boulder Canyon

Feature: Hoover Dam Penstock System

Subject: Evaluation of tie rods at the A-1 penstock junction,
Upper Arizona Penstock

Prepared: Oliver Warren Finzell Peer Review: Robert V. Zedd

Checked: Joseph P. Keelen Date: _____

TABLE OF CONTENTS

Introduction.....	1
Methods	1
Strain gage installation.....	1
Testing.....	5
Results.....	6
Accelerometers	6
Strain gages	7
Hydrodynamic Model	9
Discussion.....	12
Downstream Tie Rod	13
Upstream Tie Rod	15
Recommendations.....	18

FIGURES

Figure 1. Tie rods at the junction of A-1 penstock lateral	1
Figure 2. Machined fitting to retain pass through connector	2
Figure 3. Pass-through connector, manufactured by PAVE Technologies	2
Figure 4. Fitting welded in place on interior of penstock near base of tie rod on the A-1 lateral. Gages are in place, 90 degrees apart, at a location where the rod is threaded into the base fitting.....	3
Figure 5. Strain gage wiring connected to pass-through wiring harness. Note flex-conduit to provide mechanical protection for wiring.....	3
Figure 6. Numbering system and location for tie rod strain gages	4
Figure 7. Summary of all test runs as a function of A-1 flow versus total flow.....	6
Figure 8. Range (max-min) of acceleration versus A-1 lateral discharge for sensors located on the external stiffening plate in the axial and lateral direction.....	7
Figure 9. Stress data from gages 1, 5 , and 8 for the May tests	8
Figure 10. Frequency content of strain gage and accelerometer time series, Run 13, March 2001 tests	9

Figure 11.	Three successively more detailed models were used to generate data with Flow-3D	10
Figure 12a.	Flow-3D output showing velocity contours for the condition of 3000 ft ³ /s, flowing down the A1 lateral	10
Figure 12b.	Flow split condition , 4164 ft ³ /s total discharge..	11
Figure 12c.	All flow past the A1 lateral, 4900 ft ³ /s total	11
Figure 13.	Cross section of downstream tie rod, see figure 6 for flow orientation.	13
Figure 14.	Stresses at downstream tie rod location 5.....	13
Figure 15.	Stresses at downstream tie rod location 8.....	14
Figure 16.	Stresses at downstream tie rod location 7.....	14
Figure 17.	Modified Goodman Diagram for stresses in downstream tie rod at A-1 lateral	15
Figure 18.	Cross section of upstream tie rod, see figure 6 for flow orientation.	16
Figure 19.	Stresses at upstream tie rod location 1	16
Figure 20.	Stresses at upstream tie rod location 4	17
Figure 21.	Stresses at upstream tie rod loaction 3	17
Figure 22.	Modified Goodman diagram for the stress cycles at three locations on the upstream tie rod, A-1 lateral.....	18

TABLES

Table 1.	Location of vertical gage centerlines above threaded fitting in inches.....	4
Table 2.	Summary results of drag induced forces on tie rods from Flow3D. Forces are in lbs, positive X is down manifold (penstock), and negative Y is down lateral	12

Introduction

Preliminary findings from a risk assessment of the Hoover Penstock System showed that fatigue failure of a tie rod was one of the possible penstock failure modes. Should a tie rod fail, the consequences would be significant due to repair costs and lost power generation. There could also be immediate consequences of loss of life in the plant. In order to evaluate the fluctuating stresses due to operational cycles on the tie rods at all the lateral locations along the Hoover upper and lower penstocks, strain gages were attached directly to the tie rods at the A-1 lateral junction and were monitored during subsequent testing. This testing was recommended by the risk assessment team in order to determine the structural integrity of the tie rods.

Methods

Testing was performed on the instrumented tie rods on lateral A-1, Upper Arizona Penstock. Data were also collected externally at the tie rod location on the N-6 lateral junction. The first set of tests were completed March 12-14, 2001 and the second series May 11-13, 2001. Four strain gages had been attached to each tie rod at the A-1 location in a previous trip on the week of January 22, 2001.

Strain gage installation

Eight-350 ohm weldable strain gages were installed on the tie rods of the A-1 lateral junction at Hoover Dam (figure 1) during the week of January 22, 2001. Prior to traveling to Hoover Dam, steel fittings were machined (figure 2) to accept molded epoxy pass-through connectors manufactured by PAVE (figure 3). These connectors are designed and have been tested at pressures up to 450 lb/in² with no visible leakage.



Figure 1.- Tie rods at the junction of the A-1 penstock lateral.

One-half inch diameter holes were lanced through the 2-1/2 inch-thick penstock walls on the invert of the penstock near the tie rod fittings. The pass-through connector fittings were then welded to the inside of the penstock, figure 4. A weldable plug fitting was located over the hole on the exterior of the penstock to provide long-term sealing and shut off should a leak occur. The coal-tar epoxy coating was chipped away in the areas that gages were placed. Additional grinding was necessary in the area that strain gages were mounted along with the areas

where wire paths were routed. The pass-through wiring harness was put through a section of flexible conduit and attached to the penstock surface by conduit clamps (figure 5).



Figure 2.- Machined fitting to retain pass through connector.



Figure 3.- Pass-through connector, manufactured by PAVE Technologies.



Figure 4: Fitting welded in place on interior of penstock near base of tie rod on the A-1 lateral. Gages are in place, 90-degrees apart, at a location where the rod is threaded into the base fitting.



Figure 5: Strain gage wiring connected to pass-through wiring harness. Note flex-conduit to provide mechanical protection for wiring.

Four strain gages were attached 90-degrees apart around the circumference of each tie rod, near the base. The gages were oriented in the axial direction of the tie rod and in planes that are parallel and perpendicular to the flow in the main penstock, fig. 6. We measured the location of the centerlines of the active gage in a slightly different manner for each tie rod. The upstream tie rod had exposed threads where it joined the base fitting and the centerline was measured up from the beginning of the threads. The downstream tie rod did not have exposed threads so the centerline was measured up from the top face of the lower fitting. The measurements probably have an accuracy of about 1/8-inch due to the variable coating thickness on the rod and fitting.

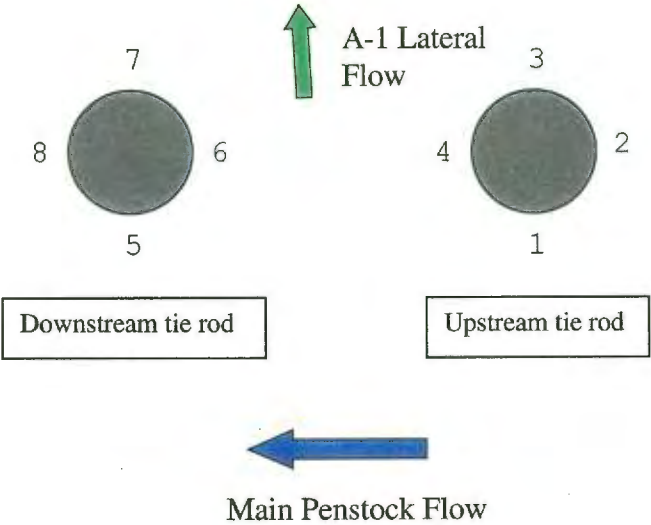


Figure 6: Numbering system and locations for tie rod strain gages.

The measured centerline locations for the strain gages are shown in Table 1

Strain gage No.	Centerline location Above fitting (in)
1	1.25
2	1.44
3	0.59
4	1.13
5	0.38
6	0.36
7	0.53
8	0.72

Table 1: Location of vertical gage centerlines above threaded fitting in inches.

Upon completion of the wiring of the strain gages, the gages and wiring were waterproofed as recommended by the gage manufacturer. Lead wire extensions were soldered on the exterior wire leads to provide cable access on the penstock walkway. After our departure, Hoover Dam personnel coated the internal area at the tie rod base with the standard paint in two applications prior to watering up the penstock.

Testing

March 12-14, 2001 - A test plan was devised that included collecting data on the internal strain gages and a number of accelerometers that were placed external to the penstock on the large stiffening plates at either end of the tie rods. The test runs basically involved setting a discharge through Unit A-1 and then increasing the downstream flows so that the total manifold flows were increased. Outputs from the strain gages and the accelerometers were acquired simultaneously for each of these specific test conditions using an IOTech Wavebook 516 with WBK11 and WBK16 add on modules. Due to maintenance activities, the maximum discharge past the A-1 lateral that we could achieve was about 4800 ft³/s.

We also installed four accelerometers on the stiffening plates at the N-6 lateral junction and recorded data for test conditions of N-6 generating 100 MW and 130 MW.

May 11-13, 2001 - At the completion of the maintenance activities that had limited test conditions in the March 2001 tests, we returned to attempt more measurements. We were now capable of having about 6250 ft³/s flow past the A-1 lateral. These flow amounts were on the order of those which had caused noticeable increases in vibration and noise levels near the lateral junctions, presumably due to some flow/tie rod interaction. The test plan covered a number of runs with essentially all discharge going through the A-1 lateral. These runs included several tests in the rough zone of unit A-1. In addition we ran several tests with high flows going past the A-1 lateral.

At the completion of these tests, we returned to the N-6 junction and took acceleration measurements on the stiffening plate for unit N-6 operating in the rough zone.

A summary of the test runs as a function of flow in A-1 versus total Upper Arizona penstock flow is shown on figure 7.

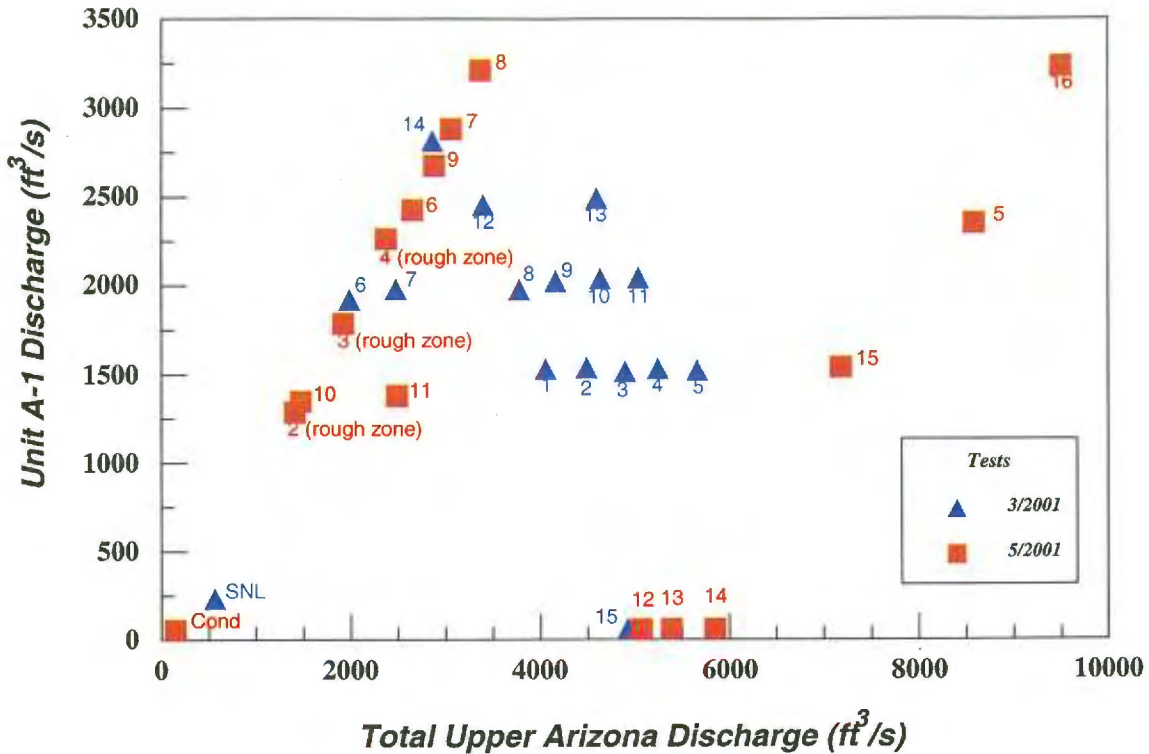


Figure 7.-Summary of all test runs as a function of A-1 flow versus total flow.

Results

Accelerometers

The accelerometer data provided information concerning the magnitudes and frequency of vibrations on the stiffening plate located external to the penstock at the tie rod ends. Accelerometers were located both on the axis perpendicular to the tie rods and also along the axis of the tie rods. As you might expect, the magnitudes along the axis of the tie rods were smaller due to the higher stiffness in that direction. Figure 8 shows both lateral and axial accelerometer responses as a function of the flow down the A-1 lateral. Test data from both the March and May tests are shown on this plot. These same data did not correlate well with total discharge. Data from the accelerometers showed no significant differences in amplitude or frequency of the vibration signal as both A-1 and N-6 were moved through the rough zone. The accelerometers did not show many lower frequencies, with the first significant frequency peak usually occurring at 48 Hz (blade passing frequency of the runner). No significant increase in vibration was noted at the N-6 junction between 100 MW and 130 MW and in fact test data collected at 90 MW showed the highest vibration amplitudes.

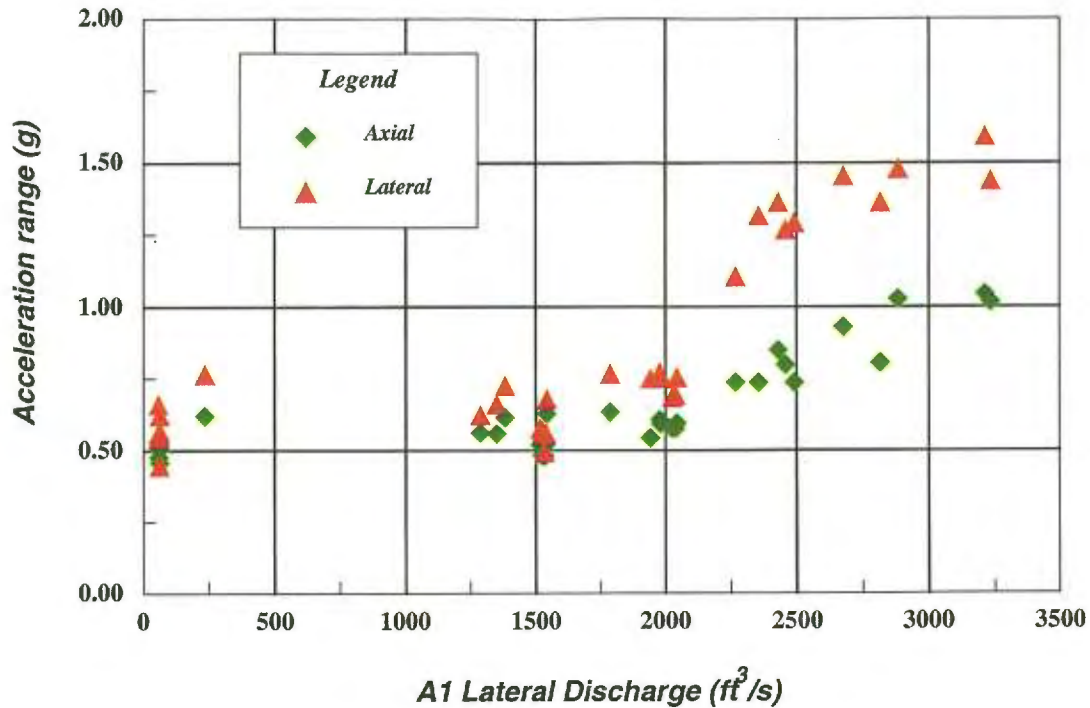


Figure 8.- Range (max-min) of acceleration versus A-1 lateral discharge for sensors located on the external stiffening plate in the axial and lateral directions.

Strain gages

The internal strain gages at the A-1 junction performed reasonably well considering the operating environment. All gages remained in place and connected to the output wiring, however some gages could not be balanced due to infiltration of water probably through the wire insulation causing decreased resistance from specimen to ground. Evaluation of the fluctuating stress ranges is important to determine potential fatigue failure due to long-term load cycling. The stress range calculated by an absolute maximum-minimum for any given run remained below 1500 lb/in² for all operating gages. The allowable stress range for the threads on the tie rods is 2170 lb/in². The measured stresses were below the allowable stress and hence there will be no fatigue crack growth. We chose the gage datum to be the case of speed-no-load for the March tests and condensing for the May tests. The actual operating stress can only be measured during a watering-up phase if gages are zeroed prior to pressurizing the penstock.

Data from the May test (fig. 9) show an approximately constant stress for discharges between 5,000 and 9,500 ft³/s for gages 5 and 8, on the downstream tie rod. Gage 5, which faces the main penstock, has a stress of -15,000 lb/in², and gage 8, at 90 degrees to 5, facing downstream to the main penstock, has a stress of -7,500 lb/in². A study of these stresses indicates that the hydrostatic loading on the tie rod, does not account for these magnitudes. The mean stress due to changes in static loads with increasing flow and decreasing pressure would be less than 300 lb/in². The stresses appear to be a result of flexure of the pipe plate in the vicinity of the tie rod. The external stiffening bar provides fixity restraint in the direction of the main penstock. Normal

to the plate there is minimal restraint afforded to the pipe in its circumferential direction. Due to flexure of the pipe, the tie rod is forced to deflect, resulting in high bending stresses.

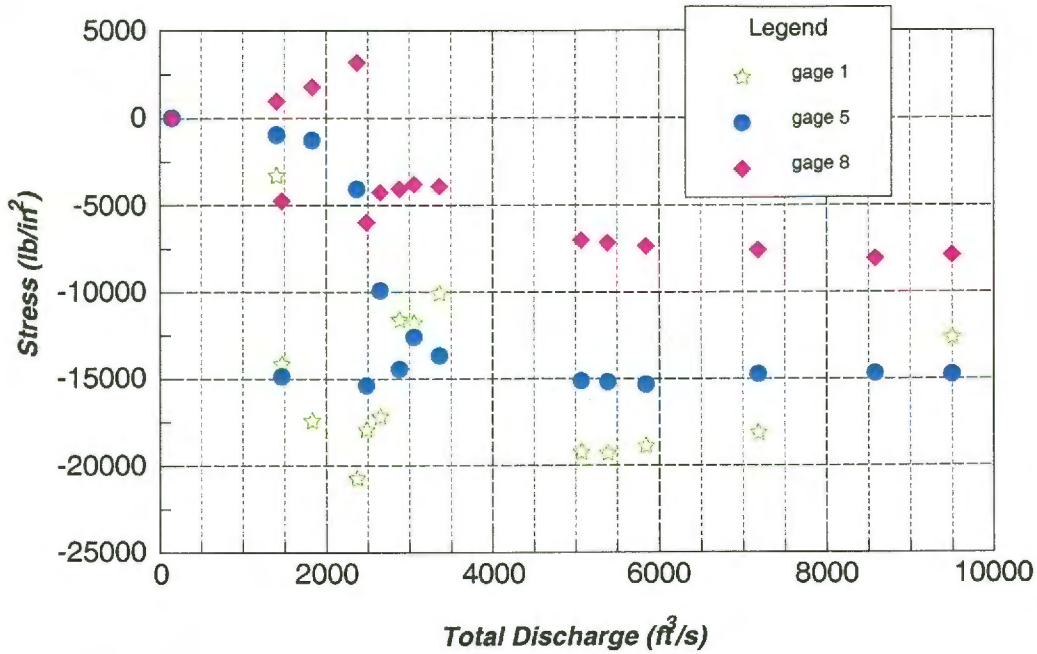


Figure 9.- Stress data from gages 1, 5, and 8 for the May tests.

In order to complete the stress analysis, we need to obtain the static stresses in the tie rod due to the internal operating pressure in the pipe. This analysis would take into account the change in the mean stresses resulting from the operation of the units, as well as the cyclic stress that occurs during the process of taking the penstock in and out of service. Indications are that we will encounter very high static stresses; possibly in the region of the tie rods yield stress. Combining high static stress values and low cycles of the mean stress could indicate a failure mode in the future.

There was some correlation between frequencies in the analysis of time series from the strain gages and accelerometers. All data were collected simultaneously. Each sensor shows correlation at a frequency of 3.8 Hz, 48 Hz, 67.6 Hz, and 96 Hz. Figure 10 shows the frequency content of strain gage 5 and accelerometer 5, up to 50 Hz. The blade passing frequency of the runner is 48 Hz.

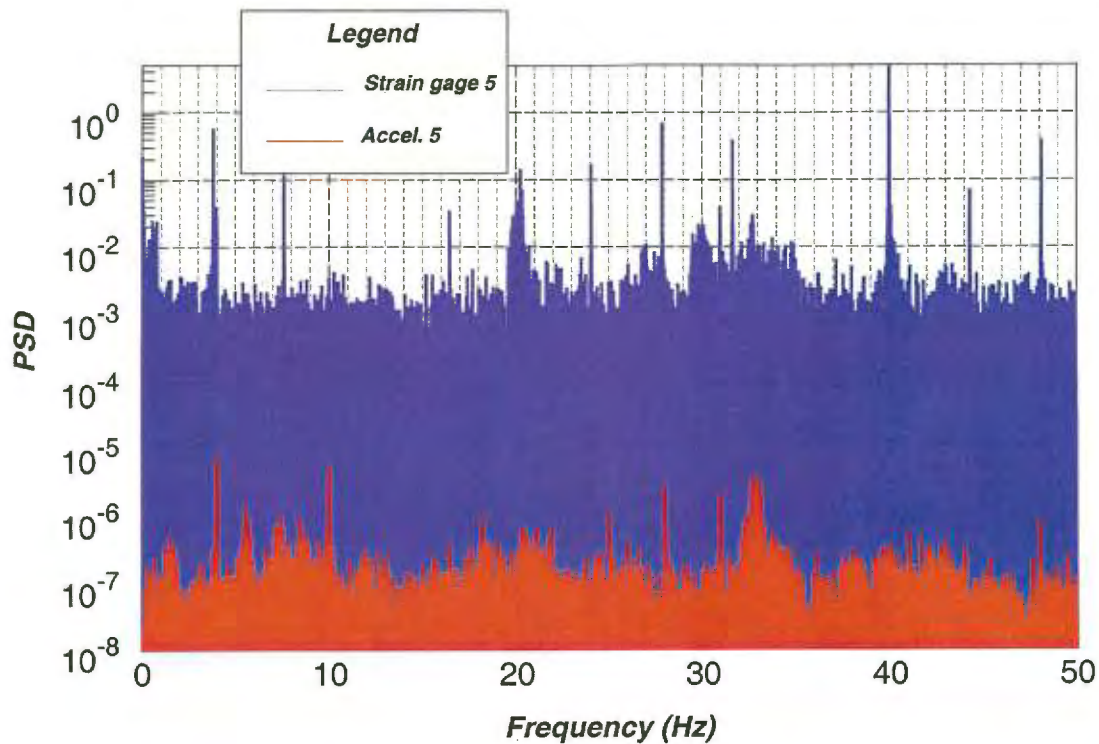


Figure 10.- Frequency content of strain gage and accelerometer time series, Run 13, March 2001 tests.

Hydrodynamic Model

As a result of some of the uncertainties concerning stress magnitudes from the testing, we carried out a math modeling effort to look at flow patterns and loadings in the vicinity of the tie rods. FLOW-3D, a three-dimensional finite volume hydrodynamic model was run for 3 different conditions at the A-1 lateral junction. Initial runs looked at a large part of the penstock system in order to generate the appropriate boundary conditions for a finer, more detailed model. In all, three iterations of the geometry were used to achieve the final results. Figure 11 shows the three geometries that were modeled. Three flow conditions were modeled that related to actual test conditions that were performed in March 2001, 1) 3000 ft³/s down the A-1 lateral and no flow down the penstock, 2) 4900 ft³/s flowing down the penstock and no flow down the A-1 lateral, and 3) a flow split between the A-1 lateral and penstock that totaled 4164 ft³/s. Some samples of the flow fields illustrating colored velocity contours are shown in Figures 12a-c. These snapshots show the complexity of the flow field around the tie rods, and show the three different flow conditions cited above for a slice at about mid-level through the lateral. Results showed that the loading on the tie rod is not uniform top to bottom. Table 2 shows results from the model for forces on the tie rod due to flow-induced drag for the three cases modeled. The CFD results give forces attributed only to drag, no loadings due to hydrostatic pressure or pipe flexure were included. Unfortunately, the numbers generated by the mathematical model did not explain the high magnitudes of stresses measured during the prototype testing.

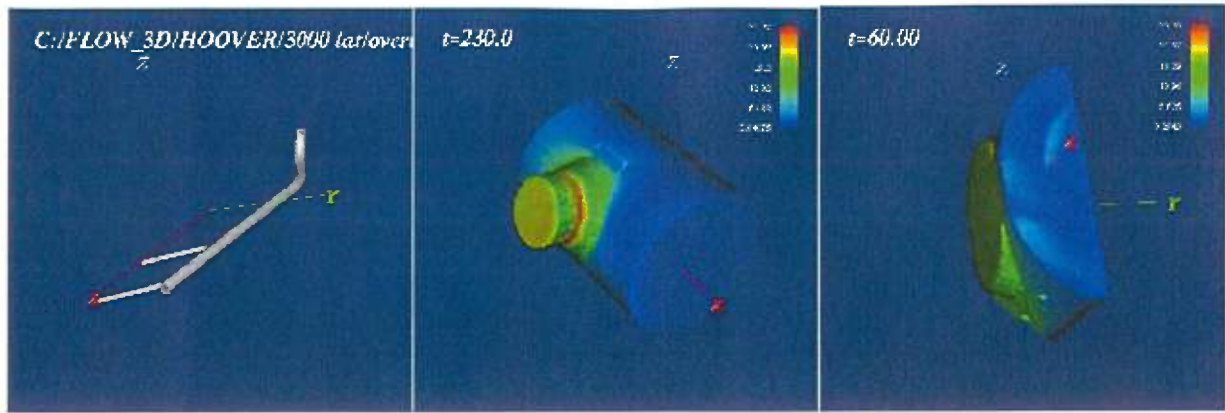


Figure 11.-Three successively more detailed models were used to generate data with Flow-3D.

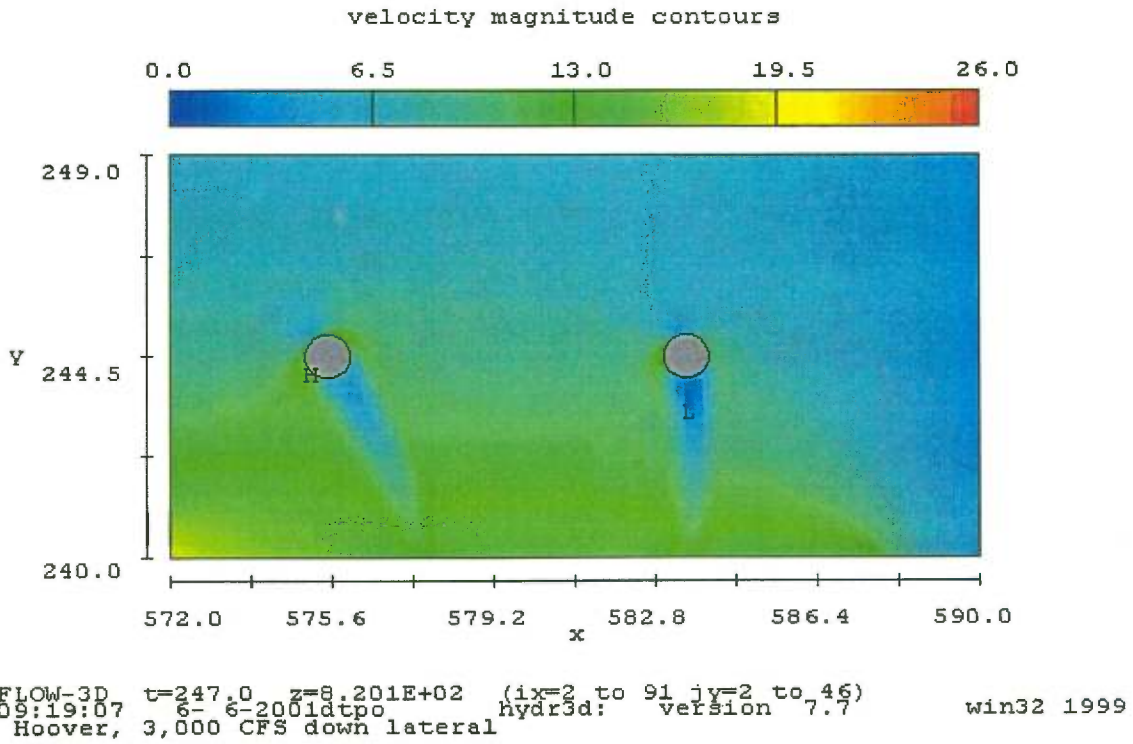


Figure 12a.- Flow-3D output showing velocity contours for the condition of 3000 ft³/s, flowing down the A1 lateral.

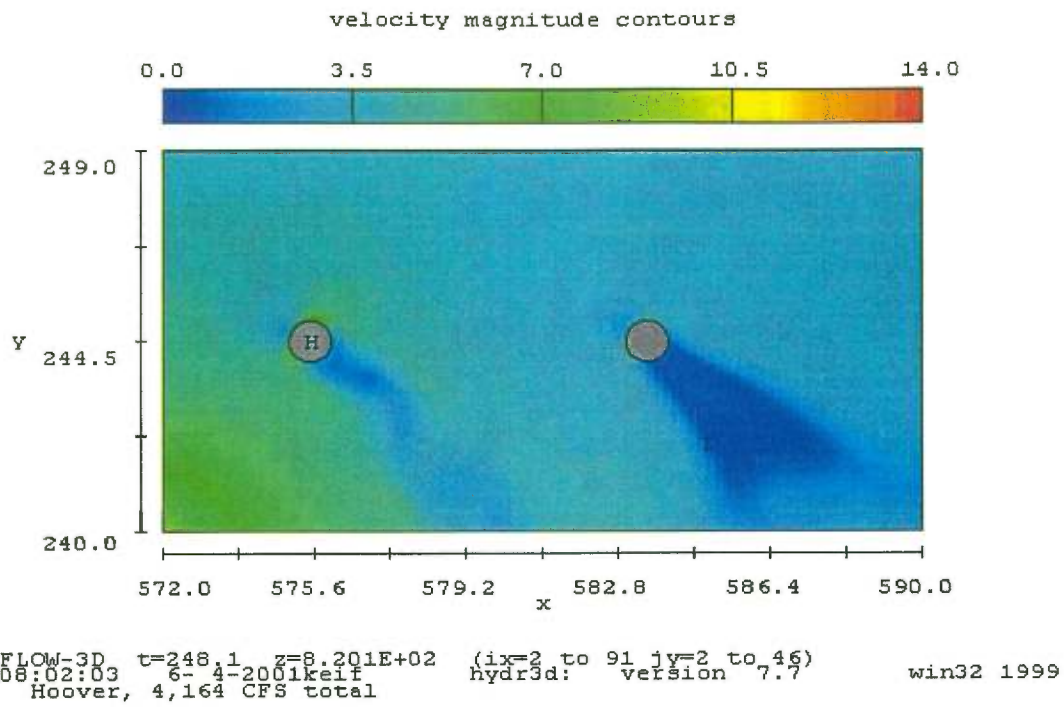


Figure 12b.- Flow split condition, 4164 ft³/s total discharge.

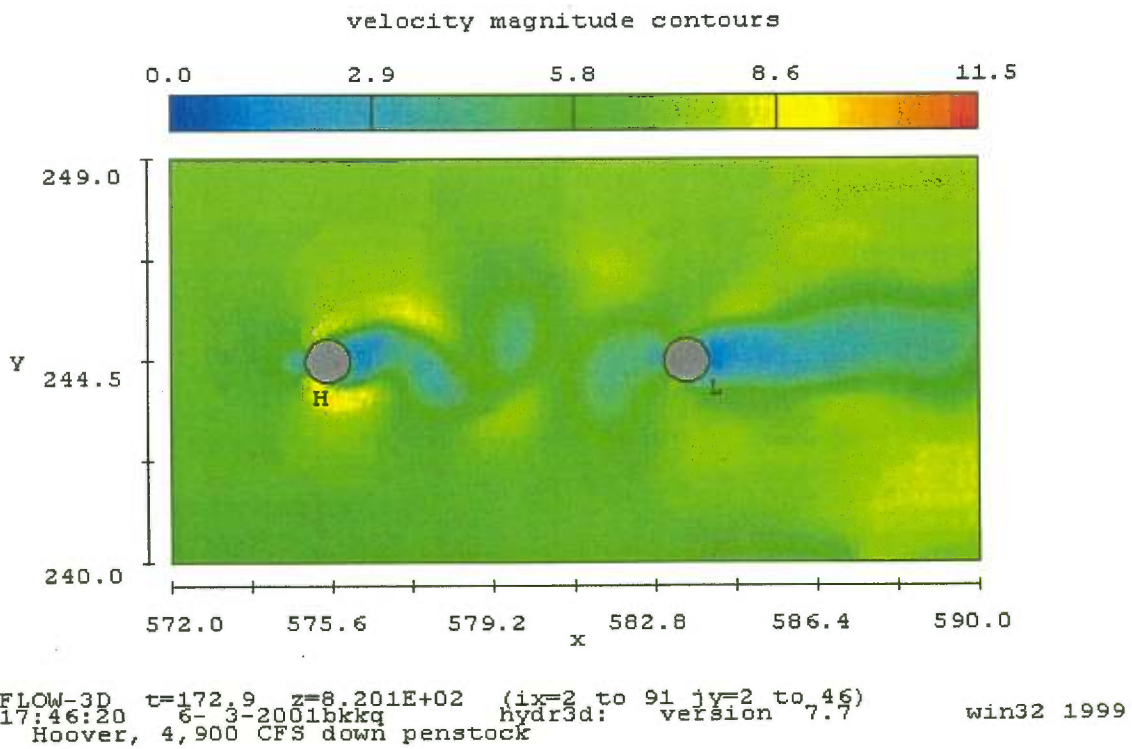


Figure 12c.-All flow past the A1 lateral, 4900 ft³/s total.

Q = 3,000 cfs down A1 lateral	
Upstream tie rod	TOTAL (lbf)
X-direction	518.14
Y-direction	-1069.17
Downstream tie rod	
X-direction	-147.267
Y-direction	-1248.43
Q =4,900 cfs past A1 lateral	
Upstream tie rod	TOTAL
X-direction	825.07
Y-direction	-55.43
Downstream tie rod	
X-direction	677.59
Y-direction	-14.87
Q =4,164 cfs flow split condition	
Upstream tie rod	TOTAL
X-direction	258.13
Y-direction	-10.15
Downstream tie rod	
X-direction	83.33
Y-direction	-32.46

Table 2: Summary results of drag induced forces on tie rods from Flow-3D. Forces are in lbs, positive X is down manifold (penstock), and negative Y is down lateral.

Discussion

From the results, the magnitudes of the operating fluctuating stresses on all operating gages were small enough to be below the threshold for fatigue. This would imply that the tie rods would have an infinite life based on fluctuating stresses generated by normal operations. This would include both excitation of the tie rods due to vortex shedding as well as that due to excitation by the power unit's major operational frequencies.

However, in addition to fluctuating stresses during operation, stress cycles also accumulate based on going from a no-flow condition to flows in excess of 5000 ft³/s and then back again to no-flow. For the purposes of this analysis, no-flow conditions in a unit include: no discharge, speed-no-load, and synchronous condensing. The operational cycle described above is assumed to occur 310 times/year. Using an operational life-to-date of 65 years, the total number of cycles thus far is 20,150. We did not measure the stress levels present in the tie rods due to pressurization of the penstock.

Downstream Tie Rod: Based on the operational stresses, we assumed a maximum stress just below yield of 34 ksi. This maximum stress will occur at location 5 (fig. 13), and is assumed to have an axial stress $f_a=18$ ksi, and a bending stress $f_b=16$ ksi. Assuming no bending occurs at 8, only an axial stress of 18 ksi will be present. Using these assumptions, the net stress at location 7 will be 2 ksi, ($f_a=18$ ksi and $f_b=-16$ ksi).

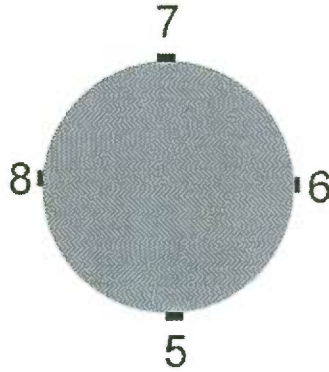


Figure 13.- Cross section of downstream tie rod, see figure 6 for flow orientation.

Data from the March 13, 2001 test showed the maximum stress at 5 was -15 ksi, and at 8 was -7.5 ksi. Assuming no bending at 8, the axial stress is -7.5 ksi and the bending stress at 5 is -7.5 ksi. Details of these operating cycles are shown in fig. 14, 15, and 16 for the locations 5, 8, and 7 respectively.

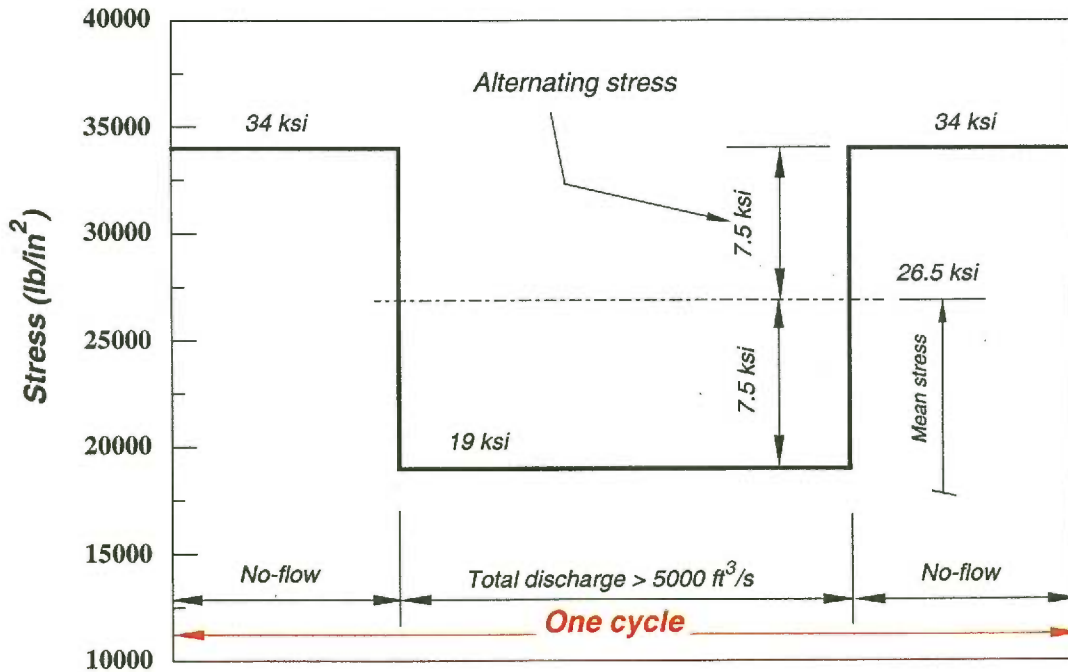


Figure 14.- Stresses at downstream tie rod location 5

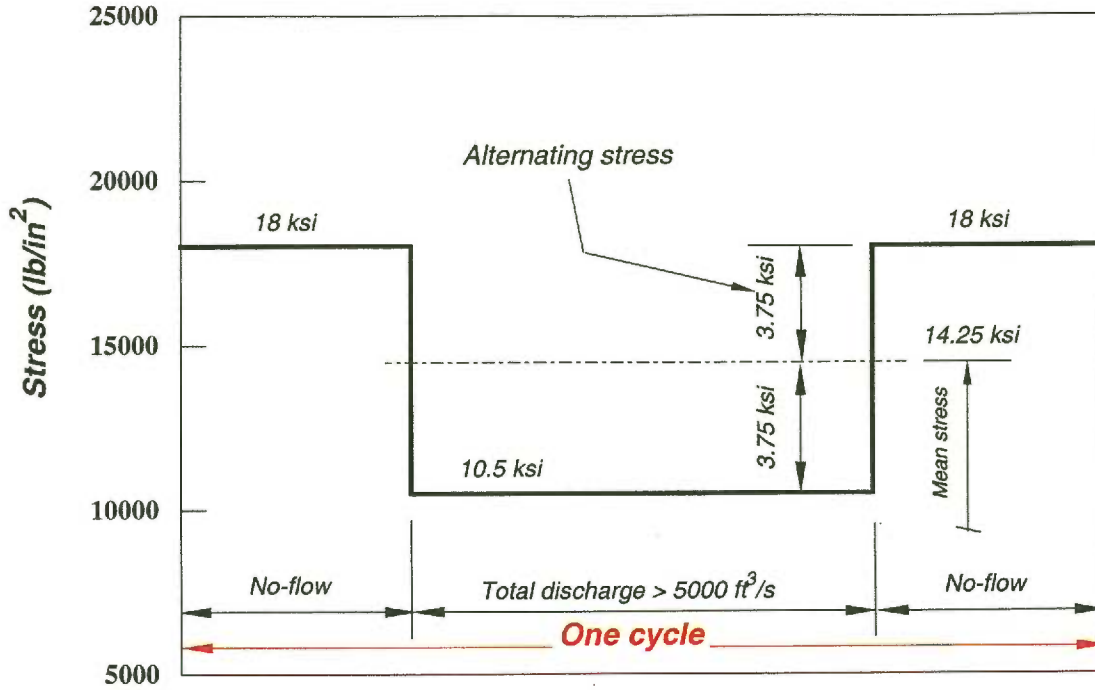


Figure 15.- Stresses at downstream tie rod location 8

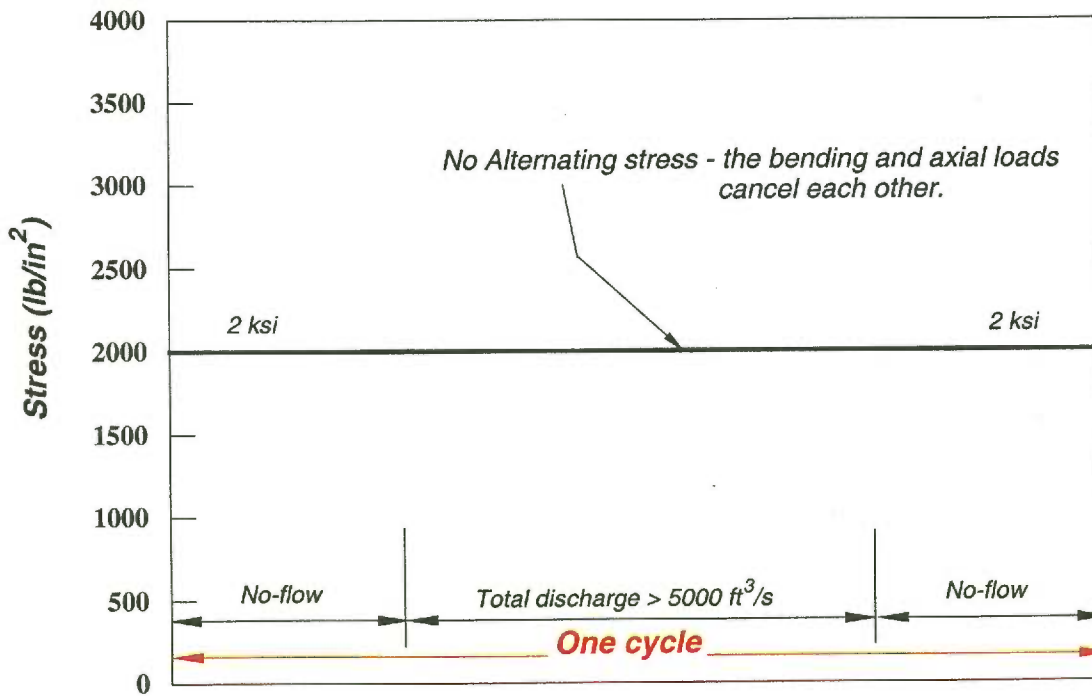


Figure 16.- Stresses at downstream tie rod location 7.

The stresses detailed here are nominal in the tie rod, and also affect the threads. Using "Recommendations For the Fatigue Design of Steel Structures," ECCS-Technical Committee-6-Fatigue, 1985, the allowable stress range for a thread with 20,150 cycles is 23 ksi, (reference Table B2.1).

The three stress cycles are shown on a Modified Goodman diagram, fig. 17. Stresses at location 5 lie outside the allowable envelope, indicating the potential for a crack to form at the first thread.

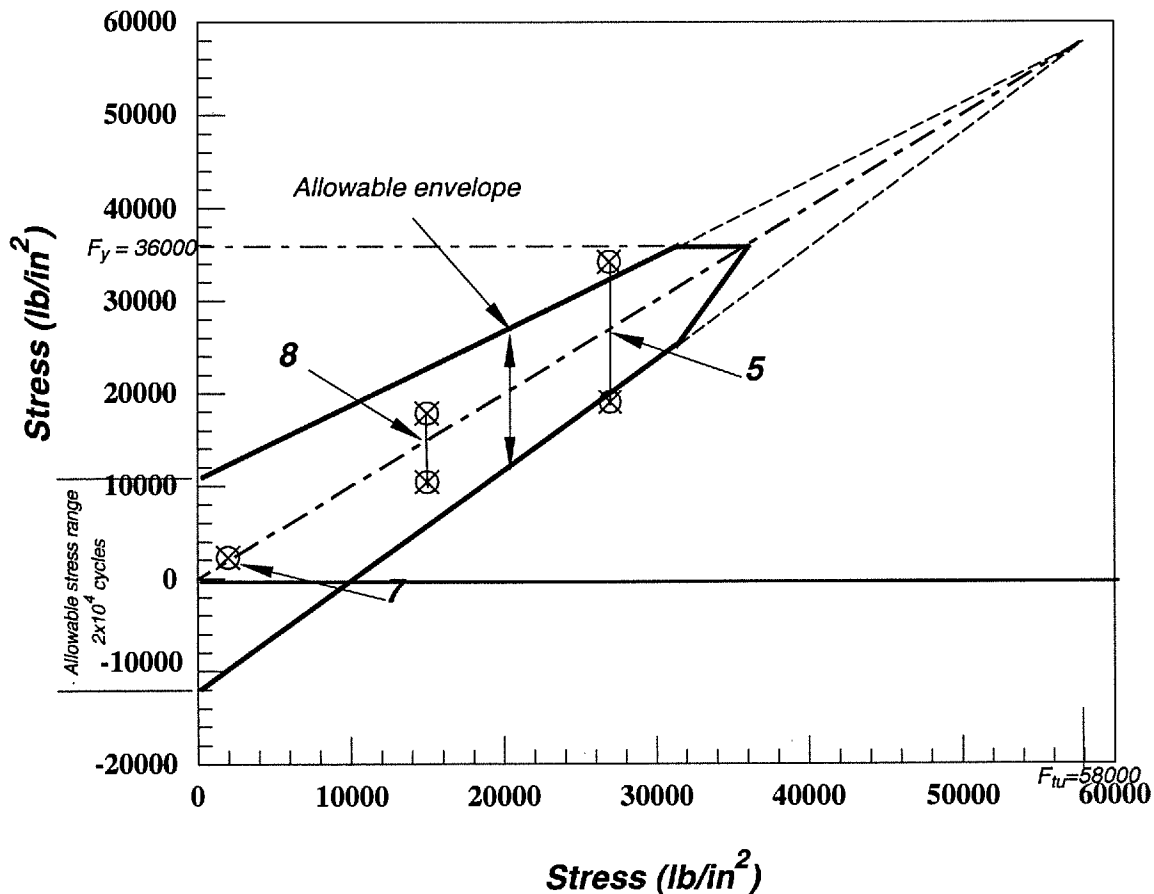


Figure 17.- Modified Goodman Diagram for stresses in downstream tie rod at A-1 lateral.

Upstream Tie Rod: The no-flow stress conditions will be assumed to be the same as those described for the downstream tie rod. Test data from March 13, 2001, showed a maximum stress of -20 ksi, occurring at location 1 (fig. 18). At location 4, the axial stress was -7.5 ksi, which resulted in a bending stress of -12.5 ksi at location 1.

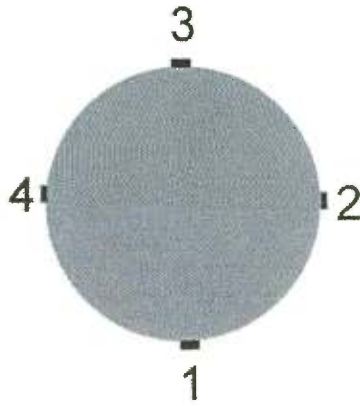


Figure 18.- Cross section of the upstream tie rod, see figure 6 for flow orientation.

The three stress cycles for the upstream tie rod locations are shown on figs. 19-21.

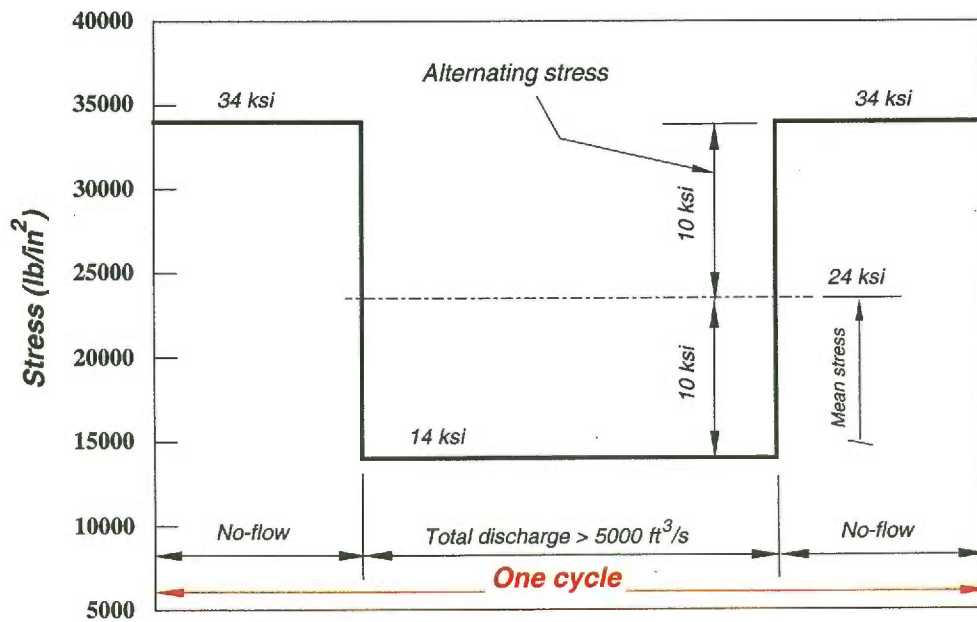


Figure 19.- Stresses at upstream tie rod location 1.

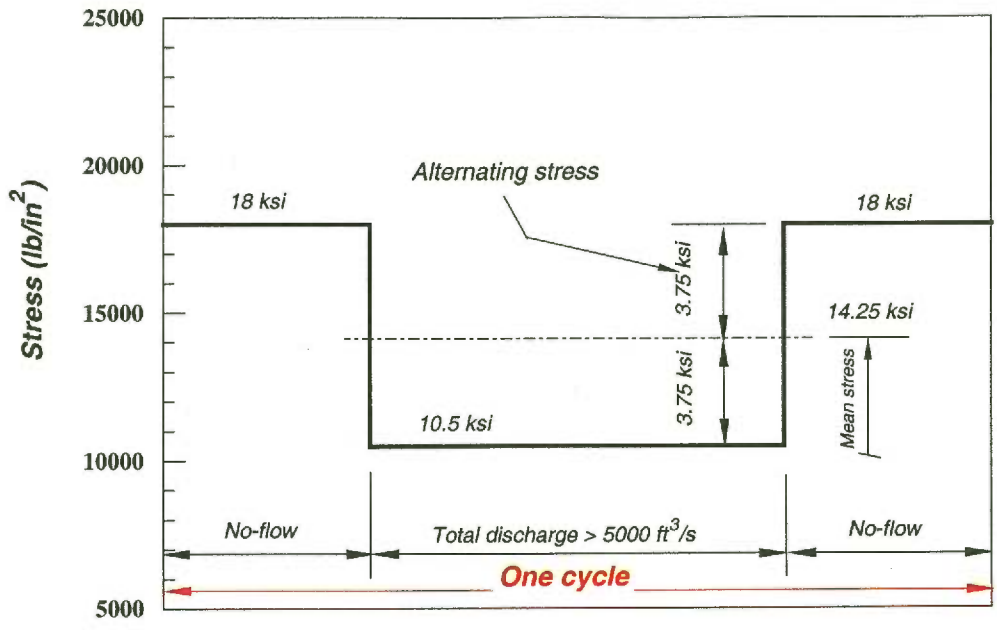


Figure 20.- Stresses at upstream tie rod location 4.

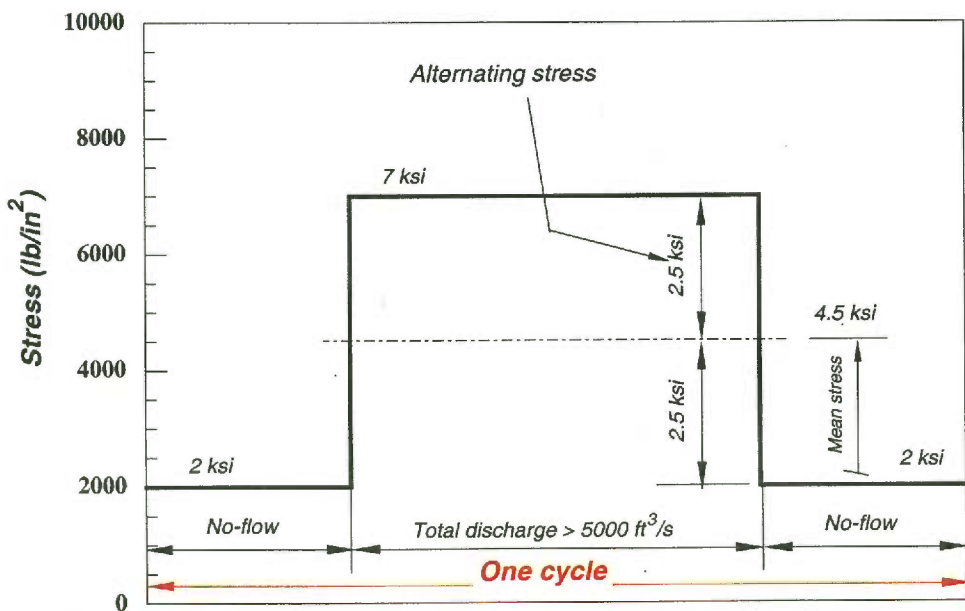


Figure 21.- Stresses at upstream tie rod location 3.

The three stress cycles are also shown on a Modified Goodman diagram, figure 22. Stresses at location 1 lie outside the allowable envelope. There is a possibility of a crack forming at the first thread below location 1.

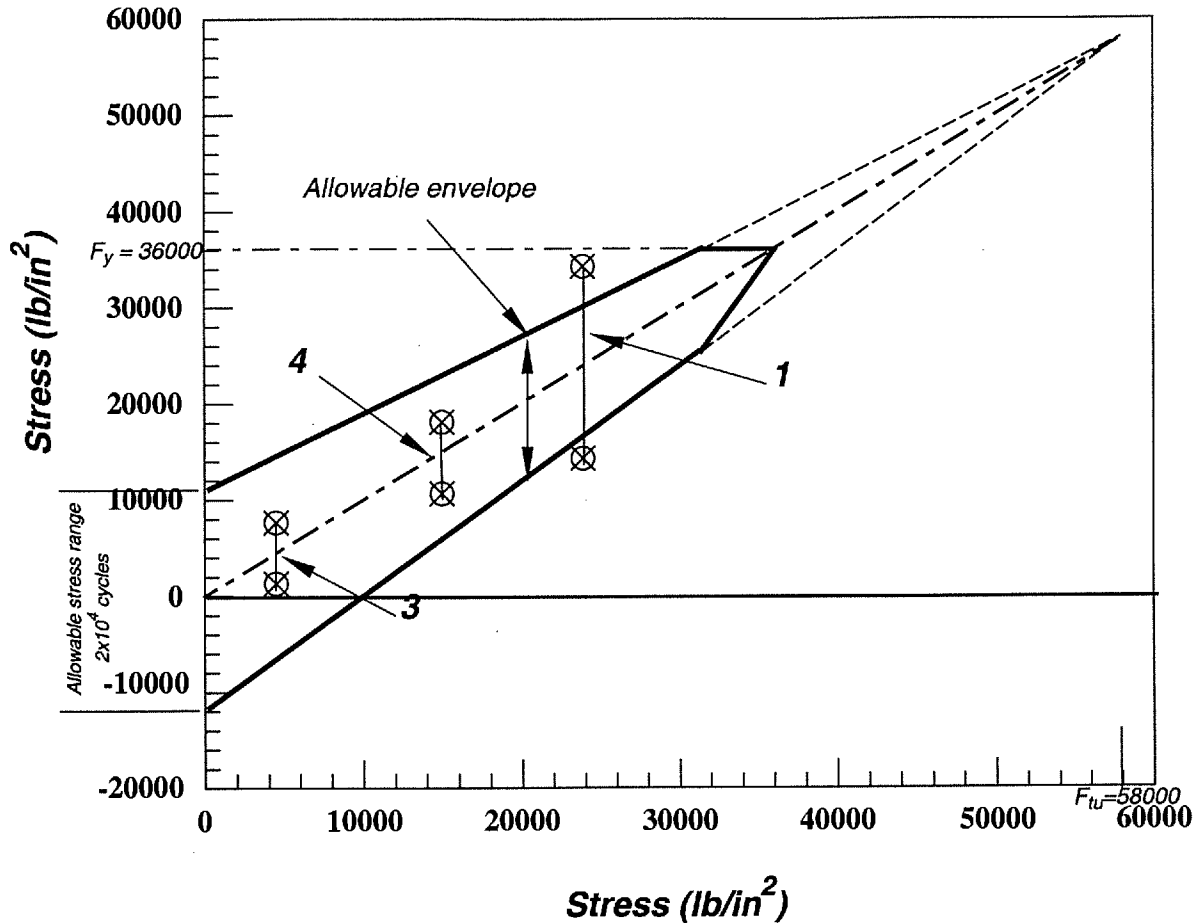


Figure 22.- Modified Goodman diagram for the stress cycles at three locations on the upstream tie rod, A-1 lateral.

Recommendations

At the next penstock outage, propose installation of strain gages on both tie rods at the most upstream lateral. The gage installation would be similar to that which was performed this year. The testing would record stresses during:

- the un-watered, installed condition (datum);
- under full hydrostatic pressure head (watered up, no flow);
- about six different operational conditions;
- return to the no-flow, hydrostatic condition;
- return to the un-watered condition.

Analysis of the data will determine whether the fluctuating mean stress, arising from the operation of the units, is large enough to affect the structural life of the tie rods. In addition, external strain gages on the penstock near the tie rod location will help in determining whether the penstock shell is deforming, causing increased loading in the tie rods.

There are no data that show good reason to restrict operation of Unit N-6. During testing at levels from SNL, through the rough zone and up to 130 MW, the highest level of vibration occurred at roughly a 90 MW load. This vibration amplitude was not significantly higher than when the unit is operating at speed-no-load. Even though there is substantial noise associated with operations that can be heard and felt along the N-6 lateral and in the area of the penstock junction, the amount of energy being imparted to the tie rods appears to be small.